Journal of Power Technologies 105 (1) (2025) 15 -- 29

Design of fuzzy power system stabilizer for improving MG dynamic

Rebin Mohammad Amini, Sajad Najafi Ravadanegh [2,✉]

[1] Energy and Environment Research Center, Shahrekord Branch, Islamic Azad University, Shahrekord, Iran
[2] Smart Distribution Grid Research Lab, Department of Electrical Engineering, Azarbaijan Shahid Madani University, Tabriz, Iran
✉ s.najafi@azaruniv.edu

Abstract

This study compares a controller based on fuzzy power system stabilizer (FPSS) with the complementary power system stabilizer (CPSS) for a microgrid (MG) containing an induction motor (IM)- diesel machine (DM) - governor (GV)- photovoltaic (PV) (IDGP). Furthermore, the linear Heffron-Phillips model is developed for MG. Using the traditional stabilizer, a specific range is calculated for changes in the MG input parameters, and a fuzzy logic controller is designed to achieve a good performance in this wide range with a high damping ratio. The simulation results of the IDGP state space model reveal that the fuzzy logic stabilizer has an excellent ability to enhance damping torque of MG dynamic, with a linear model. The IDGP small signal stability assessment is completed with oscillatory mode trajectory and Heffron-Phillips model. In this paper the control of the voltage source converter is done using sliding mode concept. The efficiency of the presented controllers on damping of critical modes is tested through time domain.

Keywords: Microgrid, dynamic stability, Heffron-Phillips model, fuzzy logic

Introduction

Systems using renewable resources, which have been increasingly employed for large power generation and the power industry are one of the most significant infrastructures in every country. Besides, PV array is discussed in many research communities around the world in recent decades [1-3]. Interest in harvesting renewable energy (RE) sources, especially the PV system to generate electricity is increasing and paving the way is a strong government support and serious concern for the environment. Due to the growth of demand, cost per output power ($/W) PV array is gradually decreased, on the other hand employment of it, becomes more possible due to governmental support [4].

Grid-connected PV power sources have been greatly brought into the traditional power systems recently; therefore, their grid connection may meaningfully affect power system dynamics and operational characteristics, including small signal stability. Because the technology of manufacturing PV cells is greatly improved, the price of the PV modules has efficiently

decreased in recent years and just as the price of conventional petrochemical fuels for power generating varies greatly [5,6].

Hence, the comprehensive utilization of PV modules with high generation electrical energies becomes more and more practical, possible, and realizable. In addition, new buildings have recently been equipped with PV array to efficiently save energy consumption of buildings, and it is mainly employed to supply remote, and isolated loads [7].

RE resource and power system applications present important new challenges for modelling and control of voltage source converter (VSC). Unlike conventional power sources, which are operated to match the demand of the loads, VSC interfaces for distributed generation, such as PV and wind, are controlled to extract the maximal power and the asynchronous process [8]. Moreover, if it is not controlled in a suitable way, it can lead to instability in the system. Various types of DG employ VSC to transform and synchronize with network systems. Analysis of the result (such as small signal stability, increment of fault current, steady state voltage) and some technical factors of installing RE resource are obligatory and should be reported to power system operators before connecting to network systems. Their impact and conclusions are represented in [8-11]. In addition, several authors for VSC have presented nonlinear mathematical models and control strategies, adaptive control, robust control and decoupling control in converter stations using feedback linearization in [12-15]. Nonlinear control techniques based on the input–output linearization with significant attainment have been developed over recent years and applied to power electronic control [16]. Many researchers showed that the PV array was excellent for utility-scale grid-connected utilization [17-19], while in [20-26] concentrated on the characteristics of utility of the interactive PV array.

In this paper, to determine the transient behaviors and stability limits of the IDGP system, with the penetrating power generation of the PV array, the dynamic-stability concept has been represented. CPSS provides sufficient damping to low frequency oscillation, although they fail in geographically distant areas. Bearing this in mind, a selection of controller location and feedback signals of controllers in a wide area network has been represented in [27], which [27,28] have proposed a methodology for selection of input and output signals, and a robust fuzzy controller is designed. Therefore, to enhance the damping ratio and dynamic stability, additional damping is generally provided by the controller using fuzzy logic controller.

System model

The single machine infinite bus power system model consists of an IM, DM, GV, PV system and a transmission line connected to an infinite bus has been shown in Figure 1. A CPSS and FPSS are applied in the excitation of the machine. Furthermore, PV system with only active power, connected to a simple infinite-bus power system with an asynchronous motor load at a PCC is illustrated in Figure 1. The voltage control is performed by the DM which is equipped with an automatic voltage regulator (AVR) and it also has GV to ensure completeness of the system.

Eq. (1) represents the amount of power extracted from the PV which depends upon the magnitude of the voltage across the capacitor Cdc (1) [29]. Therefore, various ratios of power sharing can also be achieved between the DE and the PV system.

$$p_{pv} = \left(N_p I_{ph} - N_p I_s \left[\exp\left(\frac{q v_{dc}}{N_s k_{pv} T_c A_{pv}} \right) - 1 \right] \right) v_{dc} \quad (1)$$

Nonlinear power system modeling

The dynamic behavior of the IDGP system portrayed in Figure 1 is governed by multiple nonlinear equations that are described in the rotating dq frame of reference represented as follows:

Governor model

The block diagram of the governor, as shown in Figure 2, is represented with three nonlinear mathematical models as shown in Eqs. (2) through (4) [30].

$$\frac{du_1}{dt} = \left(\frac{-1}{T_2}\right)u_1 + \left(\frac{K_1K_2}{T_2}\right)p_m \quad (2)$$

$$\frac{du_2}{dt} = u_3 \quad (3)$$

$$\frac{du_3}{dt} = A_{90}u_1 - \frac{1}{k_2}u_2 - \frac{k_1}{k_2}u_3 - A_{94}p_m \quad (4)$$

In which K T1 = 1 / 2, K T2 = 12 /12, that T1 is dead time constant and T2 is actuator time constant. Parameters K1, K2 and K3 are used for depicting the actuator, current driver and the engine torque constant, respectively.

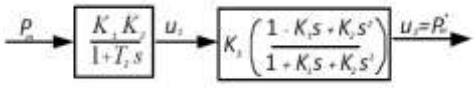

Figure 2: DM governor block diagram with Padé

Diesel model

The DM and the exciter have been modelled using the standard single axis simplified model as given in

Eqs.(∘∧)-() [31].

$$\frac{d\delta}{dt} = \omega_0(\omega - 1) \quad (5)$$

$$\frac{d\omega}{dt} = \frac{1}{2h}\left(p_m - p_e - D(\omega - 1)\right) \quad (6)$$

$$\frac{dE'q}{dt} = \frac{1}{T'_{do}}\left(E_{fd} - E'_q - (x_d - x'_d)i_d\right) \quad (7)$$

$$\frac{dE_{fd}}{dt} = \frac{1}{T_a}\left(-E_{fd} + k_{avr}\left(v_{tref} - v_t\right)\right) \quad (8)$$

PV array model

The system from the VSC to PCC, represented with nonlinear model as below [30]:

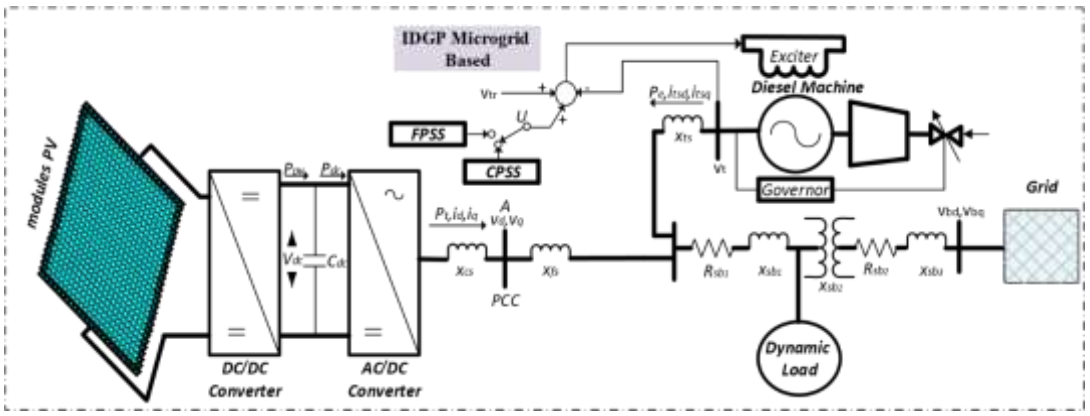

Figure 1: DM governor block diagram with Pade

$$\frac{dv_{dc}}{dt} = \frac{\omega}{c_{dc}}\left(\frac{v_{acb}}{v_{dcb}}\right)^2\left(\frac{p_{pv}}{v_{dc}} - \frac{v_d i_d}{v_{dc}} - \frac{v_q i_q}{v_{dc}}\right) \quad (9)$$

$$\frac{di_d}{dt} = \omega i_q - \frac{\omega v_d}{L_f} + \frac{m_d \omega v_{dc} v_{dcb}}{L_f v_{acb}} \quad (10)$$

$$\frac{di_q}{dt} = -\omega i_d - \frac{\omega v_q}{L_f} + \frac{m_q \omega v_{dc} v_{dcb}}{L_f v_{acb}} \quad (11)$$

The PV array converter is controlled using a second order sliding mode controller, hence, to achieve this concept, additional state variable g, is framed.

The state variable mathematical model for g, achieved from Eqs. (9) through (11) as given in Eq. (13).

$$\frac{dv_{dc}}{dt} = g \quad (12)$$

$$\frac{dg}{dt} = \frac{A_1 v_d}{v_{dc}}\left(\frac{\omega v_d}{x_{cs}} - \omega i_q - m_d v_{dc} A_2\right) + \frac{A_1 v_q}{v_{dc}}\left(\frac{\omega v_q}{x_{cs}} + \omega i_d - m_q v_{dc} A_2\right) \quad (13)$$

The SMC technique is to define a sliding surface for the variables of interest. In addition, the control philosophy SMC operates in such a way as to bring the said variables into this surface which the usual surfaces are for the error between the actual value of the variables and their reference value. To control the VSC, the state variables v_{dc} and i_q are the variables of interest, thus a sliding surface is defined for every single of these variables and the expressions for the control, md and m_q , are acquired as represented in Eqs. (14)-(15).

$$m_d = \frac{A_3 m_3 + A_4 g + A_7 v_q^2}{v_d} + \frac{A_6 v_d - A_5 i_q}{v_{dc}} + \frac{(A_5 - A_{10}) v_q i_d - A_{11} v_q^2 - A_8 g^2 - A_9 v_q m_4}{v_d v_{dc}} \quad (14)$$

$$m_q = \frac{A_{10} v_q i_d + A_{11} v_q^2 - A_9 v_q m_4}{v_d v_{dc}} \quad (15)$$

Induction motor

The nonlinear mathematical model of induction motor, which is considered as dynamic load, has been given as a three differential Eqs.(16) through (18) [31].

$$\frac{dv'_d}{dt} = -\frac{1}{T'_o}\left[v'_d + (x_s - x'_s) i_{qs}\right] + p\theta_r v'_q \quad (16)$$

$$\frac{dv'_q}{dt} = -\frac{1}{T'_o}\left[v'_q + (x_s - x'_s) i_{ds}\right] + p\theta_r v'_d \quad (17)$$

$$\frac{d\omega_r}{dt} = \frac{1}{2H}[T_e - T_m] \quad (18)$$

Heffron-Phillips modeling of power system

The nonlinear model of the IDGP system can be linearized around an operating point, thus the state space model (Ẋ= AX + BU) achieved as represented in Eq. (19), besides the operating point of the IDGP power system is acquired by running a power flow.

Where A, B, X and U are the state matrix, input matrix, the state vector and input vector, respectively.

The Heffron-Phillips model (HPM) of the IDGP MG proposed for small signal analysis and selection of damping control signal for the design of damping controller.

Furthermore, many analytical conclusions and design methods have been developed based on this model and to systematical

investigation of the damping performance of FPSS on dynamic stability, this work established the HPM of the IDGP microgrid. It demonstrated how the damping torque analysis can be performed to examine the impact of FPSS and CPSS controller on damping power system oscillation.

The HPM of the IDGP microgrid is achieved by linearizing the nonlinear Eqs. (2) through (18) and its constants are calculated based on the given values of the nominal operating point. The HPM linear block diagrams of the IDGP

$$\begin{bmatrix} \Delta\dot{u}_1 \\ \Delta\dot{u}_2 \\ \Delta\dot{u}_3 \\ \Delta\dot{g} \\ \Delta\dot{v}_{dc} \\ \Delta\dot{i}_d \\ \Delta\dot{i}_q \\ \Delta\dot{\delta} \\ \Delta\dot{\omega}_{de} \\ \Delta\dot{E}'_q \\ \Delta\dot{E}_{fd} \\ \Delta\dot{\omega}_{rind} \\ \Delta\dot{v}_d \\ \Delta\dot{v}_q \end{bmatrix} = AX + BU = \begin{bmatrix} A_{89} & 0 & 0 & 0 & 0 & 0 & 0 & 0 & 0 & 0 & 0 & 0 & 0 & 0 \\ 0 & 0 & 1 & 0 & 0 & 0 & 0 & 0 & 0 & 0 & 0 & 0 & 0 & 0 \\ A_{90} & A_{91} & A_{92} & 0 & 0 & 0 & 0 & 0 & 0 & 0 & 0 & 0 & 0 & 0 \\ 0 & 0 & 0 & A_{30} & A_{81} & A_{82} & A_{33} & A_{84} & A_{85} & A_{86} & 0 & 0 & A_{87} & A_{88} \\ 0 & 0 & 0 & 1 & 0 & 0 & 0 & 0 & 0 & 0 & 0 & 0 & 0 & 0 \\ 0 & 0 & 0 & A_{54} & A_{55} & A_{56} & A_{57} & A_{58} & A_{59} & A_{60} & 0 & 0 & A_{61} & A_{62} \\ 0 & 0 & 0 & 0 & A_{64} & A_{65} & A_{66} & A_{67} & A_{68} & A_{69} & 0 & 0 & A_{70} & A_{71} \\ 0 & 0 & 0 & 0 & 0 & 0 & 0 & 0 & \omega_0 & 0 & 0 & 0 & 0 & 0 \\ 0 & A_{72} & 0 & 0 & 0 & A_{73} & A_{74} & A_{75} & A_{76} & A_{77} & 0 & 0 & A_{78} & A_{79} \\ 0 & 0 & 0 & 0 & 0 & A_{20} & A_{21} & A_{22} & 0 & A_{23} & A_{63} & 0 & A_{24} & A_{25} \\ 0 & 0 & 0 & 0 & 0 & A_{27} & A_{28} & A_{29} & 0 & A_{30} & A_{31} & 0 & A_{32} & A_{33} \\ 0 & 0 & 0 & 0 & 0 & A_{34} & A_{35} & A_{36} & 0 & A_{37} & 0 & 0 & A_{38} & A_{39} \\ 0 & 0 & 0 & 0 & 0 & A_{40} & A_{41} & A_{42} & 0 & A_{43} & 0 & A_{44} & A_{45} & A_{46} \\ 0 & 0 & 0 & 0 & 0 & A_{47} & A_{48} & A_{49} & 0 & A_{50} & 0 & A_{51} & A_{52} & A_{53} \end{bmatrix} \times \begin{bmatrix} \Delta u_1 \\ \Delta u_2 \\ \Delta u_3 \\ \Delta g \\ \Delta v_{dc} \\ \Delta i_d \\ \Delta i_q \\ \Delta\delta \\ \Delta\omega_{de} \\ \Delta E'_q \\ \Delta E_{fd} \\ \Delta\omega_{rind} \\ \Delta v_d \\ \Delta v_q \end{bmatrix} + \begin{bmatrix} 0 & 0 & k_{u2} & 0 & k_{u4} & k_{u4} & 0 & 0 & 0 & 0 & 0 & 0 \\ 0 & 0 & 0 & 0 & & & & & & & & \\ A_{93} & 0 & A_{94} & 0 & 0 & 0 & 0 & 0 & A_{72} & 0 & 0 & -A_{72} \\ 0 & 0 & k_{u6} & k_{u7} & k_{u8} & & & & & & & \\ 0 & 0 & 0 & 0 & 0 & 0 & 0 & 0 & 0 & k_{u5} & 0 & 0 \\ 0 & 0 & 0 & 0 & & & & & & & & \end{bmatrix} \begin{bmatrix} v_{dc_{nf}} \\ v_{trf} \\ i_{g_{nff}} \end{bmatrix} \quad (19)$$

power system represented in Figure 3, it can be seen that there are 14 state variables existing in the IDGP microgrid. The dynamic stability of the microgrid is analyzed by having the HPM of Figure 3.

Design of complementary power system stabilizer

The capacity of a power system to maintain small signal stability depends highly on the PSS, hence the function of the PSS is to damp the low frequency oscillations of the generator [32]. The conventional controller PSS acts on the excitation system of the DM, hence the performance of a conventional stabilizer is limited, and it is sensitive to changes in power system parameters [33].

The DC voltage reference of the PV power plant can now be proposed as follows:

$$v_{\text{dcref}} = k_{cpss}\Delta E'_q + v_{\text{dcref}} \quad (20)$$

Where v_{dcref} is an input to the IDGP microgrid and a matrix K is defined, then augmented to the A matrix by equation $\Delta u = -K\,\Delta x$.

The input vector is written with regards to the new matrix, since their state vector and the IDGP microgrid is now shown in the state space model as represented in Eq. (21), where the eigenvalues of A_{new} show the eigenvalues of the IDGP power system with the proposed auxiliary power system with the proposed auxiliary control signal

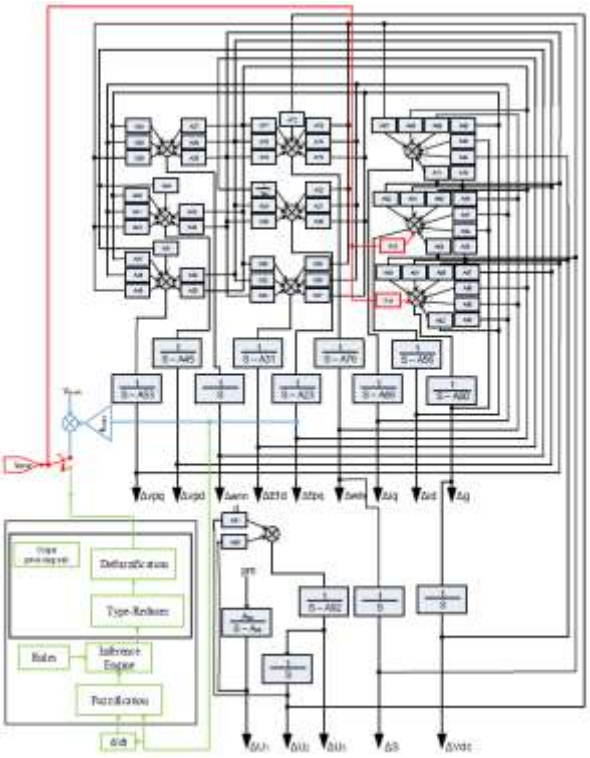

Figure 3: Phillips-Heffron model of IDGP system with FPSS and CPSS.

Fuzzy power system stabilizer (FPSS)

A fuzzy logic-based PSS gives a consistently better performance than the conventional PSS to damp low frequency oscillation and small signal stability [34]. The concept of a FPSS has been shown in Figure 4. Fuzzy logic stabilizer design includes the definition parameters which are represented as follow:

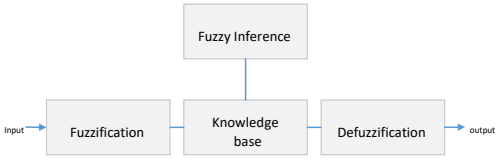

Figure 4: The concept of a fuzzy logic controller.

Fuzzification and defuzzification

Transforming the measured numerical values to the corresponding linguistic is fuzzification [35], while defuzzification is transformation after inference, a fuzzy set of a linguistic variable to numeric values [36].

Knowledge base

Knowledge base contains the description of the control membership functions. It should be noted that fuzzy membership functions are defined for each stabilizer interest variable and the necessary rules to show control objectives using linguistic variables. Furthermore, an inference mechanism must be capable of simulating researcher rule making and refers to the internal mechanism for production of output values for given input values through fuzzy rules. The designs of FPSS two inputs and one output are considered, which are changes in the DM angular speed deviation ($\Delta\omega$) and the derivation of change in DM angular speed deviation ($\Delta\omega'$) and reference voltage of VSC (v_{dcref}), respectively. It should be noted that five membership functions are considered for each input signal and output which are represented in Figure 5 and Figure 6.

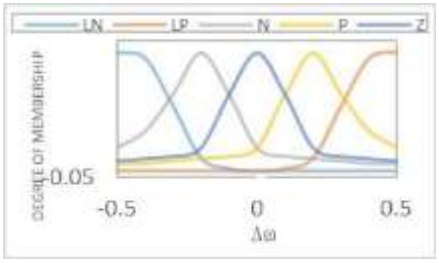

a) Membership function of Δω

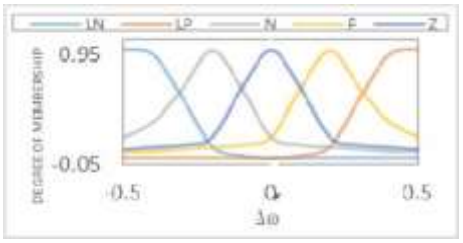

b) Membership function of Δω'

Figure 5: Membership functions of input.

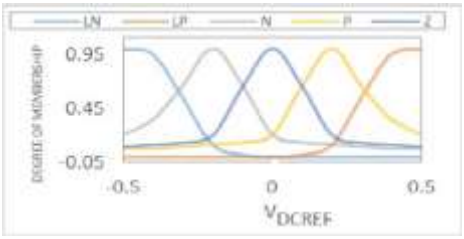

Figure 6: Membership functions of output Control Output of Fuzzy PSS.

Bases rules

Fuzzy logic controller sets are defined for each Δω, Δω' and v $_{dcref}$, hence there are five fuzzy levels (large negative (LN), negative (N), zero (Z), positive (P), large positive (LP)) and their membership functions are Gaussian that the 25 rules described presented in a matrix called matrix inference given in the Table [37].

In our method we use max–min inference that is the Mamdani method, besides the defuzzification method used in this FLC is the center of the area as given in Eq. (22).

$$U_{fpss} = \frac{\sum \quad (i = 1_i^N W\theta_i)}{\sum \quad (i = 1_i^N W)} \qquad (22)$$

Where θ1, θ2, θ3,..., θn represent the centroids of N fuzzy logic membership functions and they are assigned to Ufpss and Wi representing the firing strength of the ith rule [38].

Table 1: Inference matrix.

ω_i / ω_i'	LN	N	Z	P	LP
LN	LN	LN	LN	N	Z
N	LN	LN	N	Z	P
Z	LN	N	Z	P	LP
P	N	Z	P	LP	LP
LP	Z	P	LP	LP	LP

Simulation and results

To evaluate the effect of the FPSS and CPSS on dynamic stability, a number of simulation studies have been carried out on the IDGP microgrid.

It can be noted that the sample MG does not enjoy acceptable small signal stability when a disturbance occurs, hence performances of CPSS and FPSS on the system are discussed using the simulation. The trajectory of the electromechanical modes is shown in Figure 7, the damping of these modes at higher levels of PV power is relatively low. To improve the small signal stability at higher levels of PV power, we apply a CPSS to the IDGP system. Since the controller is given as an input to the VSC of the PV system. The trajectory of oscillatory mode with the addition of CPSS to the IDGP system is shown in Figure 8.

The sensitivity of the electromechanical modes of the system with respect to the value of k_{cpss} could be seen from the trajectories, besides with slight variation in the k_{cpss} value, the eigenvalues change drastically, and furthermore in this work the value of k has been chosen arbitrarily. In addition, with an increase in k_{cpss} , the IDGP system becomes unstable.

However, with multiple variations, a possibility exists of making the system stable at all ratios of power sharing and if one must consider all variations, then the parameters of the controller can be achieved using evolutionary algorithms with the objective as defining a specific region for the eigenvalues. According to what was said, we can use the control law Eq. (20) to resolve this problem and enhance dynamic stability of the system in all operating points. Then, according to Section 6, we apply the controller based on fuzzy logic, the results of the simulation are shown in Figure 9.

It is clear that the electromechanical modes of the IDGP have been shifted to the left and the system damping with the fuzzy logic stabilizer method greatly improved and increased in all operating conditions.

It should be noted that to achieve the effect of the controllers on the angular speed of DM, a comparison between system without PSS, system with FPSS and

system with CPSS for typical selection of gains k_{cpss} =−4.8 k_{cpss} =−5 k_{cpss} =−5.2 and k_{cpss} =−7 are given in Figure 10. The small signal stability of the IDGP system has been examined by making use of it in mechanical power input. It could be seen from Figure 10 that the proposed controller is able to damp out the oscillations. The objective of this proposed method is to stabilize the power system performance and minimize the deviation between the actual and reference field.

Furthermore, in Figure 10 it is observed that the FPSS has minimum overshoot, and the results of the simulation show that the fuzzy will produce the best response. These results confirm that it is truly the dynamic and control functions of the PV system that affect the power system small signal stability, besides compensating its effect the fuzzy logic stabilizer is a good choice, and the eigenvalue trajectory analysis has good performance to assess stability of the IDGP system.

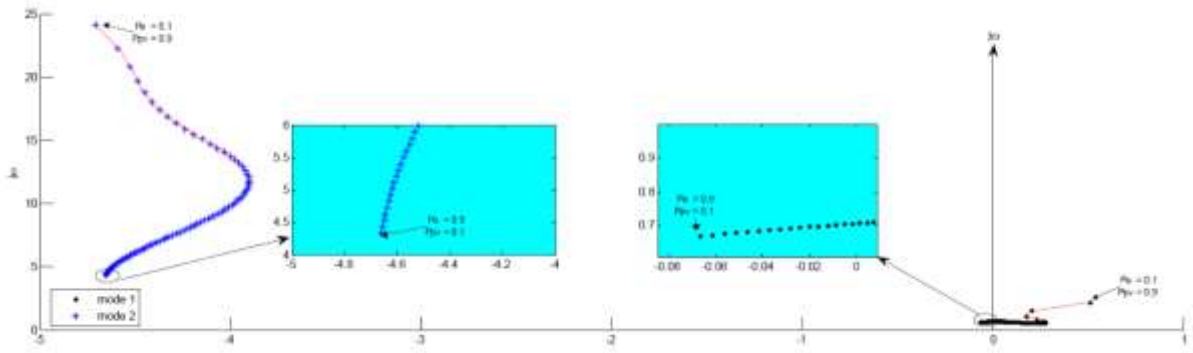

Figure 7: Oscillatory modes trajectory of the IDGP system without controller.

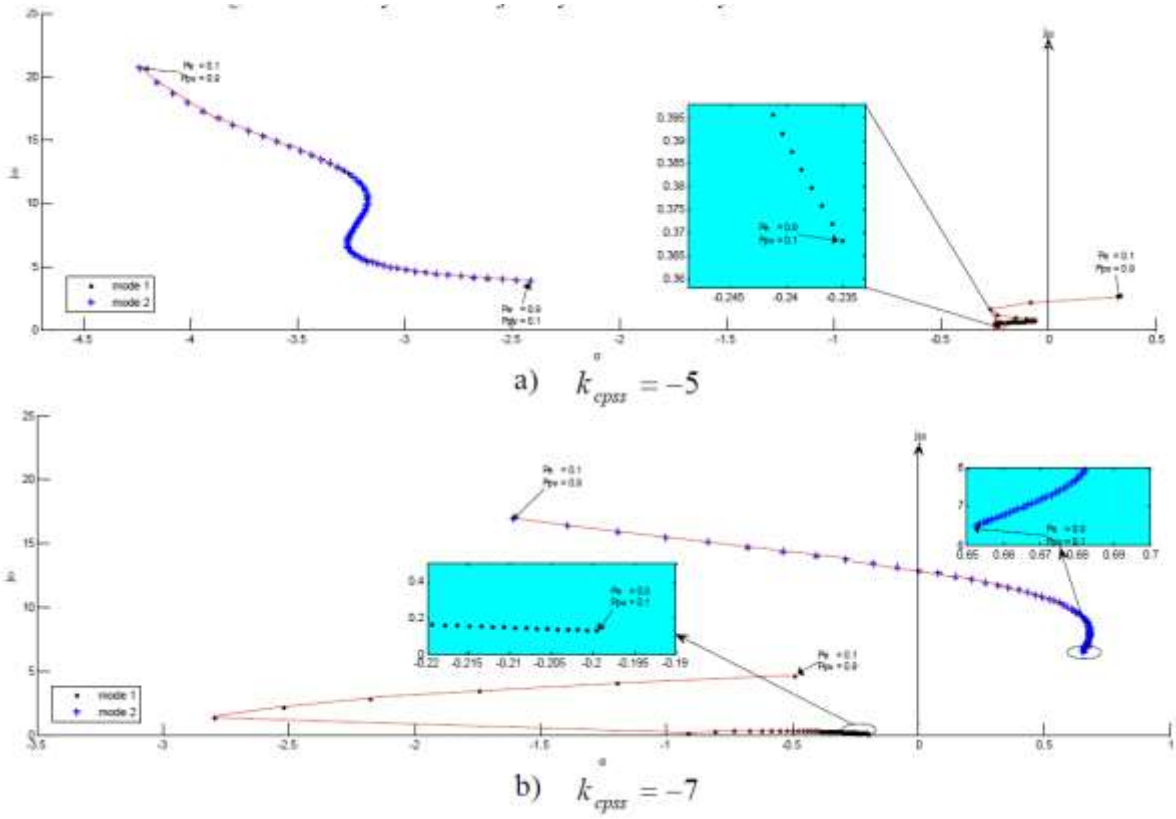

Figure 8: Oscillatory modes trajectory of the IDGP system with CPSS.

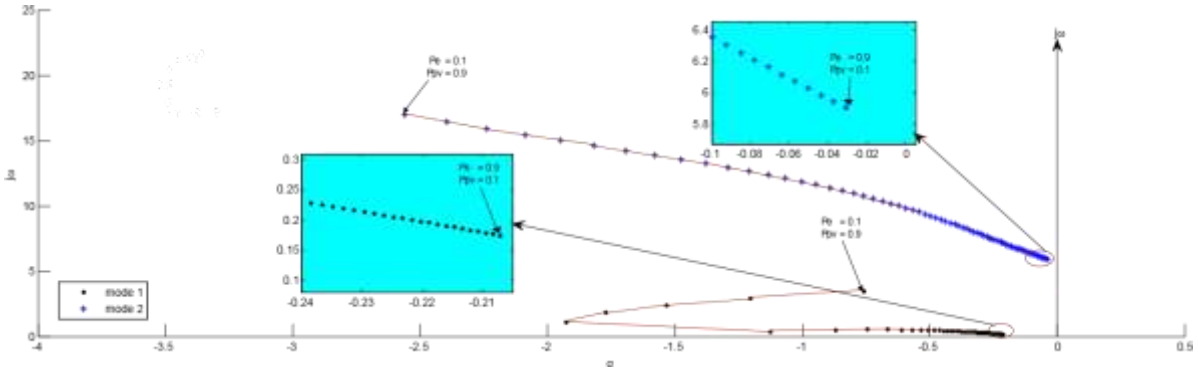

Figure 9: Oscillatory modes trajectory of the IDGP system with FPSS

Table shows the inference matrix of fuzzy controller. The IDGP single machine infinite bus system and DM governor block diagram with Padé approximation are represented in Figure 1 and Figure 2, respectively.

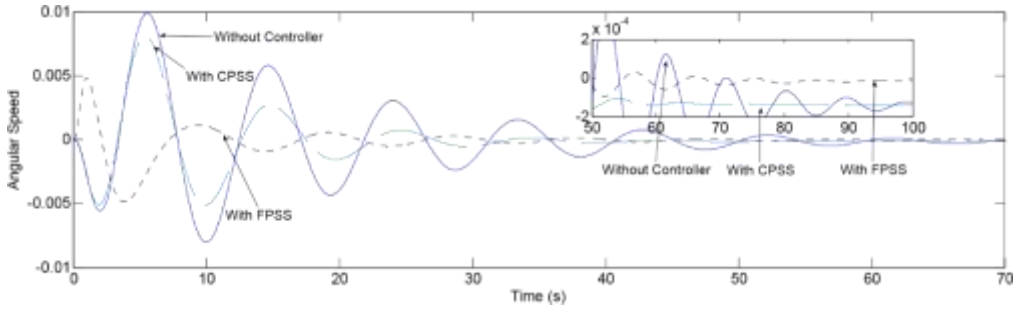

a) $k_{cpss} = -4.8$

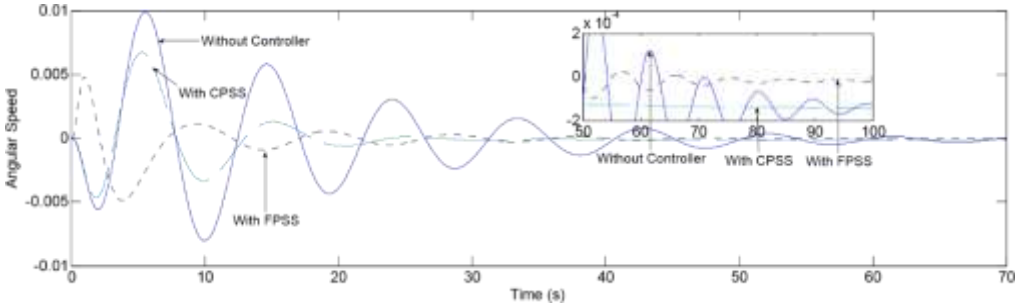

b) $k_{cpss} = -5$

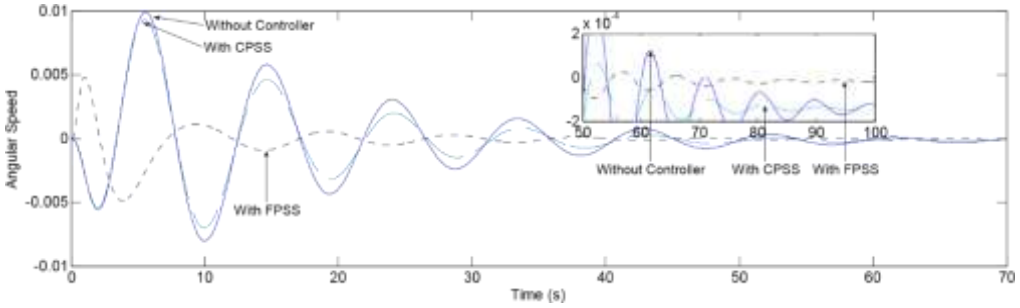

c) $k_{cpss} = -5.2$

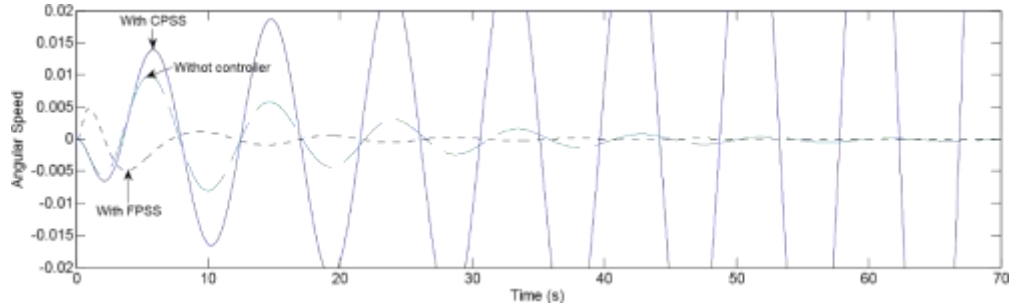

d) $k_{cpss} = -7$

Figure 10: Angular speed of diesel machine with CPSS and FPSS

The Heffron-Phillips of the IDGP system is presented in Figure 3, while Figure 4 shows the concept of a fuzzy logic controller. Membership functions of inputs are represented in Figure 5 and output membership function has been shown in Figure 6. Figure 7-10 shows the sensitivity of oscillatory modes with respect to the value of $k_{cpss\ s}$ and FPSS

Conclusion

In this paper a small signal model of a MG has been developed by linearizing the equations of the system around an operating point.

Moreover, the stability assessment of the system as penetration and variation level power photovoltaic was carried out. With the help of the small signal model and the eigenvalues trajectory, stability of the system has been evaluated, thus it has been shown that the system becomes unstable at the high level of the PV power. A comparison between the fuzzy logic stabilizer versus a conventional stabilizer has been carried out for a case of the IDGP system, where simulation results have shown that FPSS scheme still works very well when CPSS fails. Moreover, the control approach of the VSC has been done using sliding mode concept. In addition, the experimental results have emphasized the better performance of the proposed fuzzy logic controller with respect to the conventional stabilizer, over the whole operating conditions, both in regulation and tracking oscillatory modes. They also highlight how our approach outperforms the conventional stabilizer in terms of flexibility.

Abbreviations

PV array:

N_s	Number of PV cells in series
N_P	Number of strings in parallel
I_Ph, I_s	Photocurrent and dark current
q, T_c	Charge of an electron and cell temperature
k, A	Boltzmann's constant and ideal factor
P_{pv}, Pt, P_{dc}	PV array power, dc power into VSC and ac power from VSC
c_{dc}, v_{dc}	Dc link capacitor and voltage
X_{cs}, X_{fs}	Filter and connecting line reactance
id, i_q	dq frame current components of VSC
v_d, v_q	dq frame voltage components of PCC
md, m_q	dq frame components of modulation index of VSC
V_{acb}, V_{dcb}	Ac and dc side voltage base
ρ_1, ρ_2, k_g	Sliding mode controller gains
l_f	filter reactance
c_{dc}	capacitance

Diesel Engine:

P_e	Ac power from DE
X_{ts}, H	Winding reactance and inertia constant of DE
Vt, V_{tref}	Terminal voltage and reference
ω, δ	Angular velocity and torque angle
P_m	Input mechanical power
E_q', E_{fd}	Internal voltage and stator side exciter voltage
$Kavr$, T_a	AVR gain and time constant
K_1 K_2 K_3	Governor gains
$T_{1,\ T2}$	Governor time constants

$k_{1,\,k2}$	Padé approximation constants
i_{tsd} , i_{tsq}	dq axis components of current
$xd,\ x_d'$	Direct axis steady state reactance, transient reactance
T_{do}'	Open circuit time

Induction motor:

H_{ind} , T_e , T_m	Inertia, electrical torque and mechanical torque
ω_{rind} , δ	Induction motor angular velocity and slip
R_r, X_r , X_m	Induction motor resistance and inductance
$ids,\ i_{qs}$	dq axis components of current
v_d', v_q'	dq axis components of internal Voltage

Governor:

T_1	Time constant
T_2	Actuator time constant

Network:

R_{sb} X_{sb},	Resistance and reactance of line to main grid
X_{sb2}	Transformer reactance
$\|\|v_b\|\|$	Infinite bus voltage magnitude

Appendix

Expression for A:

$A_1 = wv_{acb2} / (c\ v_{dc}$ $_{dcb2})$; $A_2 = wv_{dcb} / (x\ v_{cs\ acb})$;

$A_3 = p_{c1} / (A\ A_{12})$; $A_4 = k / (A\ A_{12})$; $A_5 = w / A_2$; $A_6 = w / (x\ A_{cs2})$; $A_7 = w / (c\ x\ A_{dc\ cs2})$; $A_8 = 1/ (A\ A_{12})$; $A_9 = -(p\ x\ v_{c2\ csacb}) / (v_{dcb} w)$;

$A_{10} = (v_{acb} x_{cs}) / v_{dcb}$; $A_{11} = v_{acb} / v_{dcb}$; $A_{12} = (v_{acb} w_2) / (v_{dcb} x_{cs})$; $A_{13} = (A_5 - A_{10}) \times i_d / (v\ v_{dc\ d2})$; $A_{14} = v\ v_{q\ acb2} (i_q + v_q / x_{cs} - m\ v\ v_{q\ dc\ dcb} / (x\ v_{cs\ acb})) / (v_{dcb2} v_{dc})$; $A_{15} = v\ v_{q\ acb2} \times (v_d / x_{cs} - -i_q\ v\ m\ v_{dc\ \ d\ \ dcb} / (x\ v_{cs\ \ acb})) / (v_{dcb2} v_{dc})$.

$A_{16} = n_{40} + n_{15} + n_{56} + n43.$

$A_{17} = n_{100} + n_{28} + n_{19} + n_{33} + n11.$

$A_{18} = n_{42} + n_{14} + n_{31} + n_{21}$; $A_{19} = (A_3 + A_4 - (2A\ g\ v_8 / _{dc})) / v_d$; $A_{20} = p_4'''(x_d - x_d') / T_{do}'$; $A_{21} = p\ x_5 (_d - x_d') / T_{do}'$; $A_{22} = -m_5 (x_d - x_d') / T_{do}'$; $A_{23} = -(1 + p_4''(x_d - x_d')) / T_{do}'$; $A_{24} = p\ x_5'''(_d - x_d') / T_{do}'$; $A_{25} = p\ x_6 (_d - x_d') / T_{do}'$; $A_{26} = 1/v_t$; $A_{25} = p_6 * (x_d - x_d') / T_{do}'$; $A_{26} = 1/v_{t;}$ $A_{27} = -A_{26} * k_{avr} (-i_{tsq} p\ x_6''_{q2} + E\ x\ p_q'_{d4}''' - p\ i_4'''_{tsd} x_{d'2}) / T_a$; $A_{28} = -A\ k_{26\ avr} (-p\ x_6'''_{q2} i_{tsq} + p\ E\ x_{5\ q}'_d - p\ i_{5\ tsd} x_{d'2}) / T_a$; $A_{29} = -A\ k_{26\ avr} (m\ i_{6\ tsq} x_{q2} - m\ E_{5\ q}' x_d' + m\ i_{5\ tsd} x_{d'2}) / T_a$; $A_{30} = -A\ k_{26\ avr} * (n_{101} + n_{102}) / Ta$; $A_{31} = -1/Ta$; $A_{32} = -A\ k_{26\ avr} * (-p\ i_7''_{tsq} x_{q2} + p\ E\ x_5'''_{qd} - p\ i_5'''_{tsd} x_{d'2}) / Ta$; $A_{33} = -A\ k_{26\ avr} (-p\ x_7'''_{q2} i_{tsq} + p\ x\ E_{6\ d'q'} - p\ x_{6\ d'2} itsd) / Ta$; $A_{34} = -(p_8' \times v_d' - p\ v_{10\ q'}) / (2hind)$; $A_{35} = (-p\ v_8''_d - p\ v_{10\ q'}) / (2hind)$; $A_{36} = (m\ v_{7\ d'} + m\ v_{8\ q'}) / (2hind)$; $A_{37} = (p\ v_{8\ d'} + p\ v_9'''_{qj}) / (2hind)$.

$A_{38} = (i_{ds} - p\ v_9'_{pd} - p\ v_{11\ q'}) / (2h_{ind})$; $A_{39} = (i_{qs} - p\ v_9''_d - p\ v_{11\ q'}) / (2h_{ind})$; $A_{40} = p\ n_{10\ 103}$; $A_{41} = p\ n_{10\ 103}'$; $A_{42} = -m\ n_{8\ 103}$; $A_{43} = -p\ n_{9\ 103}''$; $A_{44} = -v_{q'}$; $A_{45} = -\left(1 - p_{96} (x_s - x_s') \right) / T_o'$; $A_{46} = -1\ w_{rind} + p\ n_{11\ 103}'$; $A_{47} = -p\ n_{8\ 103}'$; $A_{48} = -p$

$n_{8\,103}''$;$A_{49} = m\ n_{7\,103}$;$A_{50} = p\ n_{8\,103}$;$A_{51} = v_{d}'$;$A_{52} = w_{rind} - p_{9}'$ * $n_{103} - 1$;$A_{53} = -1/T_{o}' - p\ n_{9\,103}''$;$A_{54} = v\ A\ A_{dc\,2\,19}$; $A_{55} = m\ A_{d\,2} + A\ v_{2\,dc}(n_1 + n_{20} + n_{24} + n_{13})$;$A_{56} = n_8 + A_2 v\ n_{dc\,105}$;$A_{57} = n_{22} + A\ v\ n_{2\,dc\,106}$;$A_{58} = n_5 +$

$A_2 v\ n_{dc\,107;\,A59} = n_{30} + A\ v_{2\,dc}(n_{23} + n_{46})$; $A_{60} = n_{12}$

$+A\ v\ A_{2\,dc\,18;\,A61} = n_6 + A\ v\ A_{2\,dc\,17;\,A62} = n_9 + A_2$ *

$v\ A_{dc\,16}$;$A_{63} = A\ v_{2\,dc}(n_7 + n_{36})$;$A_{64} = A\ m_{2\,q} + A_2$ * $v_{\,dc}(n_{99} + n_4)$;$A_{65} = n_2 + A\ v_{2\,dc}(n_{48} + n_{26})$;$A_{66} = -wp_3 / x_{\,cs} + A\ v_{2\,dc}(n_{47} + n_{65} + n_{74})$;$A_{67} = -w$ * $m_2 / x_{\,cs} + A\ v_{2\,dc}(n_{55} + n_{59} + n_{44})$;$A_{68} = n_{52} + n_{68} + n_{82}$;$A_{69} = -wp_3' / x_{\,cs} + A\ v_{2\,dc}(n_{49} + n_{79})$;

$A_{70} = wp_4 / x_{\,cs} + A\ v_{2\,dc}(n_{61} + n_{84} + n_{67})$; $A_{71} =$

$wp\ x_4' / {}_{cs} + Av_{2\,dc}(n_{53} + n_{77} + n_{62})$; $A_{72} = 1/(2h)$.

$A_{73} = (n_{85} + n_{87)\,/\,(}2)$; h $A_{74} = (n_{92} + n_{94)\,/}\,(2)$; h

$A_{75} = (n_{96} + n_{95})/(2\,)$;$h\ A_{76} = -D\,/\,(2\,)$;$h\ A_{77} = (n_{90} + n_{91})/\,(2\,)$;$h\ A_{78} = n_{93}/(2\,)$;$h\ A_{79} = (n_{97} + n_{98})/(2\,)$;$h\ A_{80} = -AAv\ n_{1\,2\,d\,108} - 2g\ v\ A/{}_{dc}$; $_{81} = n_{109} + n_{110} - (Av\ A_{1\,d\,55} + Av\ A_{1\,q\,64})/v_{dc} + g_2 / v_{dc2}$;$A_{82} = n_{50} + n_{51} + n_{54} - AAv\ n_{1\,2\,d\,105} + n_{57} + n_{58} - AAv\ n_{1\,2\,q}(_{48} + n_{26})$;$A_{83} = n_{60} + n_{63} + n_{66} - AAv\ n_{1\,2\,d\,106} + n_{64} + n_{68} - AAv\ n_{1\,2\,q\,74}$;

$A_{84} = n_{71} + n_{70} - AAv\ n_{1\,2\,d\,107} + n\ A_{72}$; $_{85} = 2w$ *

$(A_{15} + A_{14)\,-}\ A\ v\ n_{12\,d}(23 + n_{46)\,-}A\ v\ n_{12\,q\,82}/$

$(Av_{2\,dc);\,A86} = n_{75} - AA_{1\,2}v\ A_{d\,18} + n_{76} + n_{73} -$

$AAv\ n_{1\,2\,q}(49 + n_{79})$; $A_{87} = n_{80} + n_{78} - A_1 \times$

$Av\ A_{2\,d\,17} + n_{81} + n\ A_{89}$; $_{88} = n_{86} + n_{83} -$

$AAv\ A_{1\,2\,d\,16} + n_{104} + n\ A_{88}$; $_{89} = -1/T2.$

$A_{90} = K\ k_3 / {}_2 + K\ k\ T\ k_{3\,1} / (2_{\,2)\,+}\ K\ T_3 / {}_{22.}$

$A_{91} = -1/\ k\ A_2$; $_{92} = -k\ k\ A_1 / {}_2$; $_{93} = k\ k\ T_{1\,2} / {}_{2.}$

$A_{94} = -(k\ K\ K\ K_{1\,1} \times {}_{2\,3} / (T\ k_{2\,2)\,+}\ K\ K\ K\ T_{1\,2\,3} / {}_{22})$.

References

[1] Solano J., Duarte J., Vargas E., Cabrera J., Jácome A., Botero M., Rey J.: Dynamic model and control of a photovoltaic generation system using energetic macroscopic representation. International Journal of Emerging Electric Power Systems. 2016 Oct 1;17(5):575-82.

[2] Ebrahim MA., AbdelHadi HA., Mahmoud HM., Saied EM., Salama MM.: Optimal Design of MPPT Controllers for Grid Connected Photovoltaic Array System. International Journal of Emerging Electric Power Systems. 2016 Oct 1;17(5):511-7.

[3] Aouchiche N., Becherif M., HadjArab A., Aitcheikh MS., Ramadan HS., Cheknane A.: Dynamic Performance Comparison for MPPT-PV Systems using Hybrid Pspice/Matlab Simulation.
International Journal of Emerging Electric Power Systems. 2016 Oct 1;17(5):529-39.

[4] Natthaphob N.: Inverter-based photovoltaic distributed generations: Modeling and dynamic simulations. In: TENCON 2010-2010 IEEE Region 10 Conference; 2010; 7-12.

[5] Schaefer J.C.: Review of photovoltaic power plant performance and economics. IEEE Trans. Energy Conversion 1990; 2: 26-37.

[6] Moore T.: Thin films: Expanding the solar marketplace. EPRI Journal 1989; 2: 4-15.

[7] Moore T.: On-site utility applications for photovoltaics. EPRI Journal 1991; 2: 26-37.

[8] Burgos R., Jian S. S.: Guest Editorial: Special Issue on Modeling and Control of Power Electronics for Renewable Energy and Power Systems. Emerging and Selected Topics in Power Electronics. IEEE Journal 2014; 4: 713-714.

[9] Freitas W., Vieira J. C. M., Morelato A., Silva L. C. P., Costa V. F., Lemos F. A. B.: Comparative analysis between synchronous and induction machines for distributed generation applications. IEEE Trans Power Systems 2006; 21: 301-311.

[10] Nimpitiwan N., Heydt G. T., Ayyanar R., Suryanarayanan S.: Fault Current Contribution from Synchronous Machine and Inverter Based Distributed Generators. IEEE Trans. Power Delivery 2007; 22: 634-641.

[11] Sedghisigarchi K., Feliachi A.: Dynamic and Transient Analysis of Power Distribution Systems with Fuel Cells - Part II: Control and Stability Enhancement. IEEE Trans. Energy Conversation 2004; 2: 429-434.

[12] Thallam R. S., Suryanarayanan S., Heydt G. T., Ayyanar R.: Impact of interconnection of distributed generation of electric distribution systems- a dynamic simulation perspective. In: Presented at Power Engineering Society General Meeting; 2006; IEEE. pp. 8-pp.

[13] Zhang G., Xu Z.: Steady-state model for VSC based HVDC system and its controller design. In: Proc IEEE Power Eng. Soc Winter Meeting; 2001; pp. 1085–1090.

[14] Ruan S. Y., Li G. J., Jiao X. H., Sun Y. Z., Lie T. T.: Adaptive control design for VSC-HVDC system based on back stepping approach. Elect. Power Syst Res 2007; 5–6: 559–565.

[15] Durrant M., Werner H., Abbott K.: Synthesis of multi-objective controllers for a VSC HVDC terminal using LMIs. In: Proc IEEE Conf. Decision and Control; 2004; pp. 4473–4478.

[16] Zhang G. B., Zexel., Wang G. Z.: Steady state model and its nonlinear control of VSC-HVDC system. Proc. CSEE 2002; 1: 17–22.

[17] Aravindan D., Ilango G. S., Nagamani C., Sai A. V. S. S. R.: Power oscillation damping using UPFC in automatic power flow control mode with constant power reference. In: Proc Int Conf Power and Energy System; 2008; Baltimore, MD, pp. 144– 149.

[18] Bzura J. J.: The New England electric photovoltaic systems research and demonstration project. IEEE Trans Energy Conversion 1991; 2: 284-289.

[19] Hoffner J. E.: Performance of Austin's 300-kilowatt photovoltaic power plants. In: Proceedings of the Biennial Congress of the International Solar Energy Society; 1991; Denver, Colorado, USA. pp. 119124.

[20] Ranade S.J., Prasad N.R., Omick S, Kazda L.F.: A study of islanding in utility-connected residential photovoltaic systems, Part I – Models and analytical methods, Part II – Case studies. IEEE Trans Energy Conversion 1989; 3: 436-445: 446- 452.

[21] Hoff T., Shugar D.S.: The value of grid-support photovoltaics in reducing distribution system losses. IEEE Trans Energy Conversion 1995; 3: 569-576.

[22] Giraud F., Salameh Z. M.: Analysis of the effects of a passing cloud on a grid-interactive photovoltaic system with battery storage using neural networks. IEEE Transactions Energy Conversion 1999; 4: 1572-1577.

[23] Middlebrook R.D., Cuk S.: A general unified approach to modelling switching-converter power stages. In: IEEE Power Electronics Specialists Conference; 1976; pp. 18-34.

[24] Hatziadoniu C. J., Chalkiadakis F. E., Feiste V. K.: A power conditioner for a grid-connected photovoltaic generator based on the 3-level inverter. IEEE Trans Energy Conversion 1999; 4: 1604-1610.

[25] Abouzahr I., Ramakumar R.: An approach to assess the performance of utility-interactive photovoltaic systems. IEEE Trans Energy Conversion 1993; 2: 145-153.

[26] Vachtsevanos G.: Simulation studies of islanded behavior of grid connected photovoltaic systems. IEEE Trans. Energy Conversion 1989; 2: 177-183.

[27] Padhy B. P., Srivastava S. C., Verma N. K.: Robust wide area TS fuzzy output feedback controller for enhancement of stability in multi machine power system. IEEE Syst J 2012; 3: 426–435.

[28] Fang DZ., Yang X., Bao S.: Design of UPFC fuzzy logic damping controller using the strategy of oscillation energy descent. International Journal of Emerging Electric Power Systems. 2006 Aug 28;6(2):1-6.

[29] Hussein K., Muta I., Hoshino T., Osakada M.: Maximum photovoltaic power tracking: an algorithm for rapidly changing atmospheric conditions. Generation, Transmission and Distribution, IEE Proceedings 1995; 1: 59 –64.

[30] Mohammad Amini R., Safari A., Najafi Ravadanegh S.: Optimal model of PDIG based microgrid and design of complementary stabilizer using ICA. ISA transactions September 2016, 64: 328–341.

[31] Anderson P., Fouad A.: Power System Control and Stability. 2nd ed. New Delhi, India, USA: Wiley, 2008.

[32] Kundur P.: Power System Stability and Control, MacGraw-Hill, 1994.

[33] Bounou M.: Contribution a l'exploitation robuste des reseaux electriques par la methode de taguchi. Thesis, Polytechnique, Montréal. 1997.

[34] Hassan M. A. M., Malik O.P., Hope G. S.: A Fuzzy Logic Based Stabilizer for a Synchronous Machine. IEEE Trans on Energy Conversion 1991, 3: 407413.

[35] Bandal V., Bandyopadhyay B., Kulkarni A. M.: Output Feedback Fuzzy Sliding Mode Control Technique Based Power System Stabilizer (PSS) For Single Machine Infinite Bus (SMIB) System. In: IEEE conference publication; 2005; pp. 341– 346.

[36] Hilal M., Errami Y., Benchagra M., Maaroufi M.: Fuzzy Power control for doubly fed induction generator-based wind farm. Journal of Theoretical and Applied Information Technology 2012; 2: 321330.

[37] Yazdchi M. R., Boroujeni S. M. S.: Power System Stabilizer Design Based on Model Reference Robust Fuzzy Control. Research Journal of Applied Sciences, Engineering and Technology 2012; 8: 852-858.

[38] Kolabi A., Sofalgar S., Lotfi T., Yousefi M.: Comparing the Power System Stabilizer Based on Sliding Mode Control with the Fuzzy Power System Stabilizer for Single Machine Infinite Bus System (SMIB). Research Journal of Applied Sciences, Engineering and Technology 2012; 1: 16-22.